

Lipid Lateral Organization on Giant Unilamellar Vesicles Containing Lipopolysaccharides

Jakubs Kubiak,^{†‡} Jonathan Brewer,^{†§} Søren Hansen,[¶] and Luis A. Bagatoli^{†§*}

Supporting Material

Section 1. Labeling LPS with Alexa fluor 488 hydrazide

LPS from *E. coli* O55:B5 (smooth) was labeled with Alexa Fluor 488 hydrazide according to a protocol described by Luk et al. (1). LPS was oxidized with 10 mM NaIO₄ in 100 mM carbonate buffer pH 5 for 20 minutes at 4°C. The reaction was stopped by addition of glycerol to final concentration of 15 mM. Oxidized LPS was purified by dialysis in 3.5 kDa cut-off Slide-A-Lyzer Dialysis Cassette (Pierce, Rockford, IL). Conjugation with Alexa Fluor 488 hydrazide was performed by overnight incubation in 10 mM phosphate buffer 150 mM NaCl pH 7.4 at 4°C. Labeled LPS was purified by size exclusion chromatography on Sephadex G-100 (Sigma-Aldrich). Purification was validated by performing fluorescence correlation spectroscopy (FCS) experiments (2), where the diffusion of single LPS molecules was measured below their critical micellar concentration ($D_{\text{coeff}} = 26.0 \pm 1.5 \mu\text{m}^2\text{s}^{-1}$, different to that measured for free Alexa Fluor 488 hydrazide, i.e. $D_{\text{coeff}} = 430 \mu\text{m}^2\text{s}^{-1}$ (3)). In order to evaluate the degree of LPS labeling, photon counting histogram (PCH) analysis was applied to our FCS data (data not shown) using the Globals software package developed at the Laboratory for Fluorescence Dynamics at the University of California at Irvine. The analysis of PCH allows one to extract information about molecular brightness (number of photon counts per molecule) and the average number of molecules in microscope focal volume (4). FCS experiments were done in samples containing known concentration of free Alexa Fluor 488 hydrazide or Alexa Fluor 488 -labeled LPS. After data analysis the molecular brightness of Alexa488 hydrazide and Alexa488 hydrazide conjugated LPS were compared at the same conditions. These experiments had shown a LPS-to-Alexa Fluor 488 labeling ratio of 1:3 mol.

Section 2. LAURDAN GP function and two photon excitation LAURDAN GP measurements

2.1 LAURDAN GP function

The fluorescence emission properties of LAURDAN are sensitive to the water dipolar relaxation process that occurs in the probe's environment, and the LAURDAN GP denotes the position of the probe's emission spectrum (5). The energy of the excited singlet state progressively decreases when the extent of dipolar relaxation process is augmented. The extent of water dipolar relaxation observed in highly packed membrane regions (e.g. the solid-ordered phase in bilayers) is very low compared to what it is observed in less packed regions (e.g. the liquid-disordered phase in bilayers). For example when a solid-ordered/liquid-disordered phase transition occurs in the membrane, a prominent red shift in the fluorescence emission spectrum of the probe is observed (from blue to green; almost 50 nm shift) (5). The GP function was defined analogously to the fluorescence polarization function as:

$$GP = \frac{I_B - I_R}{I_B + I_R} \quad (1)$$

where I_B and I_R correspond to the intensities at the blue and red edges of the emission spectrum (440 and 490 nm) using a given excitation wavelength (5-7). At equilibrium conditions, this function is sensitive to the local phase state of the membrane (8).

2.2 Two photon excitation LAURDAN GP measurements

The LAURDAN GP measurements were performed in a custom built two photon excitation fluorescence microscope described previously (9). The objective used in the experiments was a 60X water immersion objective with an NA of 1.2 (Olympus). The excitation light source was a femtosecond Ti:Sa laser (Broadband Mai Tai XF-W2S with 10 W Millennia pump laser, tunable excitation range 710-980 nm, Spectra Physics, Mountain View, CA) and the excitation wavelength was 780 nm. The excitation light was circularly polarized to avoid photoselection effects in the image plane. In order to calculate the LAURDAN GP function, the fluorescence signal from the sample was split in two different channels using a dichroic mirror (splitting at 475 nm). Each channel contains one bandpass filters (438 ± 12 nm and 494 ± 10 nm, that correspond respectively to I_B and I_R in Eq. 1). The LAURDAN GP images were calculated using the program SimFCS (Laboratory for Fluorescence Dynamics, University of California at Irvine, USA). Corrections using the G factor were performed according to Brewer et al (9), using a 160 μ M LAURDAN solution in DMSO as a reference (GP=0.006 at room temperature). The GP values obtained in the GUVs experiments (Figure 5) are computed from the distinct membrane regions using a ROI routine. Approximately 20-25 GUVs per each concentration are analyzed and the average GP reported. The LAURDAN GP measurements for the reference solution and oligolamellar vesicles were done in a fluorometer (ISS Chronos, Champaign, IL, USA) using a 374 nm diode as excitation wavelength, and 440 nm and 490 nm (I_B and I_R respectively in Eq. 1) as emission wavelengths. The GP function in these experiments was calculated using the Vinci analysis software (ISS, Champaign, IL, USA) according to Eq. 1.

Section 3. Fluorescence correlation spectroscopy of LPS-A488

The FCS measurements were performed in a custom built two photon excitation fluorescence microscope previously described in (9). The objective used in the experiments was a 60X water immersion objective with an NA of 1.2 (Olympus, UPlanSApo 60x/1.20W). The excitation light source was a femtosecond Ti:Sa laser (Broadband Mai Tai XF-W2S with 10 W Millennia pump laser, tunable excitation range 710-980 nm, Spectra Physics, Mountain View, CA) and the excitation wavelength was 930 nm. The signal was collected through a bandpass filter of 525 ± 25 nm using a photomultiplier (Hamamatsu H7422P-40). The measurements were taken using SimFCS (Globals software package developed at the Laboratory for Fluorescence Dynamics at the University of California, Irvine). The autocorrelation function (ACF) of temporal fluorescence intensity fluctuation was calculated using Eq. 2,

$$G(\tau) = \frac{\langle \delta F(t) \delta F(t + \tau) \rangle}{\langle F(t) \rangle^2} \quad (2)$$

where $\delta F(t) = F(t) - \langle F(t) \rangle$. For the FCS experiments aimed to measure the diffusion of monomeric LPS in solution, concentrations of 1 to 10 nM of Alexa488-labeled LPS in 10 mM phosphate buffer 150 mM NaCl pH 7.4 were used. Calculated ACFs were globally fitted using Globals for Spectroscopy (Globals software package developed at the Laboratory for Fluorescence Dynamics at the University of Illinois at Urbana-Champaign) to the model of single species of molecules diffusing in 3-dimensional Gaussian Two-Photon excitation volume (Eq. 3),

$$G(\tau) = \frac{\gamma}{N} \left(1 + \frac{8D\tau}{\omega_{3DG}^2} \right)^{-1} \left(1 + \frac{8D\tau}{z_{3DG}^2} \right)^{-\frac{1}{2}} \quad (3)$$

where D is diffusion coefficient, γ is instrumental factor, N is an average number of fluorescent particles in excitation volume, ω_{3DG} and z_{3DG} are the radii of the excitation volume in the xy -plane and the z -direction, respectively (2).

Diffusion of LPS was also measured in GUVs. In these experiments GUVs were prepared using unlabelled LPS doped with Alexa488-labeled LPS (~100:1 molar ratio). The laser beam was focused on the polar region GUVs. Approximately 20 vesicles per sample were analyzed. Calculated ACF was fitted to the model of single species of molecules diffusing in 2-dimensional Gaussian Two-Photon excitation volume (Eq. 4),

$$G(\tau) = \frac{\gamma}{N} \left(1 + \frac{8D\tau}{\omega_{2DG}^2} \right)^{-1} \quad (4)$$

where D is diffusion coefficient, γ is instrumental factor, N is an average number of fluorescent particles in excitation volume, ω_{2DG} is the radius of the excitation volume in the xy -plane (2).

Section 4. Estimation of the sub-microscopic domain size

The equivalent of Einstein-Stokes equation for 3D diffusion in 2D systems, is described by the Saffman- Delbrück model (10):

$$D_{coeff} = \frac{k_B T}{4\pi\mu_m h} \left(\ln \left(\frac{\mu_m h}{\mu_w R} \right) - 0.5772 \right) \quad (5)$$

where h is thickness of the membrane, μ_m is viscosity of the membrane, μ_w is viscosity of surrounding solution, and R is the radius of diffusing cylindrical object. The validity of Saffman-Delbrück model was confirmed for particles of relatively small radii (transmembrane proteins: R

of 0.5-4 nm) (11), as well as for much larger objects (microscopic-size domains: R of 0.5-10 μm) (12).

Using this model, the diffusion coefficients of LPS-Alexa488 measured from FCS experiments were used to estimate the size of these nanoscopic domains. The set of parameters describing the membrane properties (see Eq. 5) used in our calculations is: $h = 4$ nm (and 2.1 nm for single LPS molecule, which spans only half of the bilayer), $\mu_M = 180$ mPa·s, $\mu_W = 1.003$ mPa·s, $k_B T = 4 \cdot 10^{-21}$ J. Particularly, the membrane viscosity (μ_M) was estimated using the diffusion coefficient of single LPS and their known radius (a radius of 0.7 nm and a molecular area of 1.53 nm² assuming molecules with cylindrical shape (13)). We found that this membrane viscosity value is on the range of already reported values for a fluid membrane (14). The dependence of diffusion coefficient with the object size (radius) and number of molecules (assuming circular domain shape) is shown in Fig. S3. The computed values for each diffusion coefficient are showed in Table S1. Using our microscope resolution (which is ~ 380 nm in the x-y plane) we estimated that clustering of $>1 \times 10^6$ molecules per leaflet is needed in order to visualize the LPS smooth (or Ra) enriched domains. In all cases (see table S1) the estimated domain size is below our microscopy system resolution limit, observation that is in agreement with our experimental data.

References:

1. Luk, J. M., Kumar, A., Tsang, R., and Staunton, D. 1995. Biotinylated Lipopolysaccharide Binds to Endotoxin Receptor in Endothelial and Monocytic Cells. *Anal. Biochem.* 232:217-224.
2. Müller, J. D., Chen, Y., and Gratton, E. 2003. Fluorescence correlation spectroscopy. *Meth. Enzymol.* 361:69-92.
3. Jameson, D.M., Ross, J.A. and Albanesi, J.P. 2009. Fluorescence Fluctuation Spectroscopy: Ushering in a New Age of Enlightenment in Cellular Dynamics. *Biophys Rev.* 1:105-118.
4. Chen, Y., Müller, J. D., So, P. T., and Gratton, E. 1999. The Photon Counting Histogram in Fluorescence Fluctuation Spectroscopy. *Biophys. J.* 77:553-567.
5. Parasassi, T., E.K. Krasnowska, L.A. Bagatolli, and E. Gratton. 1998. Laurdan and Prodan as Polarity-Sensitive Fluorescent Membrane Probes. *J Fluoresc.* 8:365-373.
6. Parasassi, T., G. De Stasio, A. d'Ubaldo and E. Gratton. 1990. Phase fluctuation in phospholipid membranes revealed by Laurdan fluorescence. *Biophys. J.* 57:1179-1186.
7. Parasassi, T., G. De Stasio, G. Ravagnan, R. Rusch and E. Gratton. 1991. Quantitation of lipid phases in phospholipid vesicles by the generalized polarization of Laurdan fluorescence. *Biophys. J.* 60:179-189.
8. Bagatolli, L. A. 2006. To see or not to see: Lateral organization of biological membranes and fluorescence microscopy. *Biochim. Biophys. Acta.* 1758:1541-1556.
9. Brewer, J., J. Bernardino de la Serna, K. Wagner and L.A. Bagatolli. 2010. Multiphoton excitation fluorescence microscopy in planar membrane systems. *Biochim. Biophys. Acta.* 1798:1301-1308.
10. Saffman P. G., and M. Delbrück. 1975. Brownian motion in biological membranes. *Proc. Natl. Acad. Sci. U.S.A.* 72:3111 -3113.
11. Ramadurai S., A. Holt, V. Krasnikov, G. van den Bogaart, J. A. Killian, and B. Poolman. 2009. Lateral Diffusion of Membrane Proteins. *J. Am. Chem. Soc.* 131:12650-12656.
12. Cicuta P., S. L. Keller, and S. L. Veatch. 2007. Diffusion of Liquid Domains in Lipid Bilayer Membranes. *J. Phys. Chem. B.* 111:3328-3331.
13. Wiese A., M. Münstermann, T. Gutschmann, B. Lindner, K. Kawahara, U. Zähringer, and U. Seydel. 1998. Molecular Mechanisms of Polymyxin B-Membrane Interactions: Direct Correlation Between Surface Charge Density and Self-Promoted Transport. *J Membr Biol.* 162:127-138.
14. Gambin Y., R.Lopez-Esparza, M. Reffay, E. Sierecki, N.S. Gov, M.Genes, R.S. Hodges and W. Urbach. 2006. Lateral mobility of proteins in liquid membranes revisited. *Proc. Natl. Acad. Sci. U.S.A.* 103:2098 -2102.

Table S1.

Sample	$D_{\text{coeff}} (\mu\text{m}^2\text{s}^{-1})$	R (nm)	Number of molecules
LPS Alexa488	5.43 ± 0.62	0.71	1
LPS smooth 7 mol%	2.73 ± 0.28	1.7	7
LPS smooth 12 mol%	1.36 ± 0.23	32	2100
LPS Ra 9 mol%	1.99 ± 0.36	8	130
LPS Ra 12 mol%	0.98 ± 0.21	73.8	11200

Supplemental Figure legends

Fig. S1. (A) Size exclusion chromatography elution profiles of oligolamellar vesicles prepared using the full incorporation protocol (described in the methods section). The vesicles were prepared by mixing LPS smooth/*E. coli* lipids with two fluorescence probes, i.e. 0.1 mol % rhodamine-DHPE (●) and 1 mol % of LPS-Alexa488 (○). (B) Control obtained by mixing rhodamine-DHPE labeled oligolamellar vesicles containing *E. coli* lipids with pure LPS aggregates containing LPS-Alexa488 (showing that pure LPS aggregates are separated from the oligolamellar vesicles). FRI account for fluorescence relative intensity.

Fig. S2. GUVs composed of *E. coli* polar lipid extract and LPS-Alexa488. The GUVs were prepared in 10 mM TrisHCl pH 7.4, 0.15M NaCl. Fluorescence images (false color representation of Alexa488 conjugated with LPS smooth) shows incorporation of LPS into GUVs. LPS concentration in the membrane is on the order of 0.1–0.01 mol %. Scale bars are 10 μm .

Fig. S3. Dependence of the diffusion coefficient on the size (radius and number of molecules, log scale) of a diffusing object according to Saffman-Delbrück model (solid line, see section 4). The measured diffusion coefficient for LPS (smooth and Ra) at different concentrations are included in the graph.

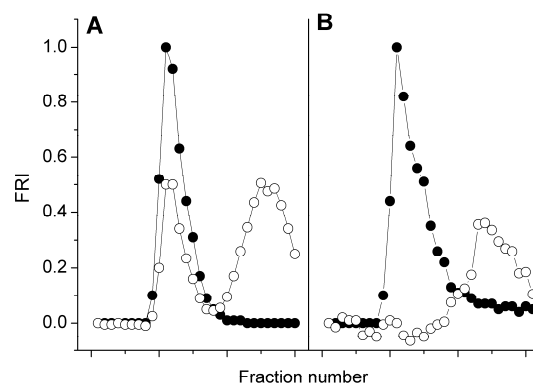


Figure. S1.

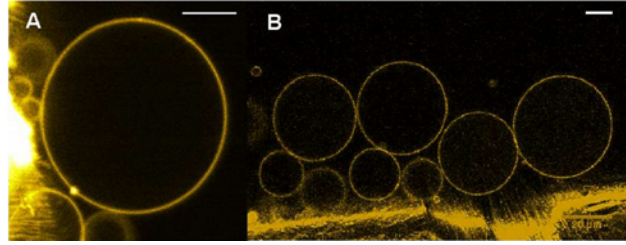


Figure S2

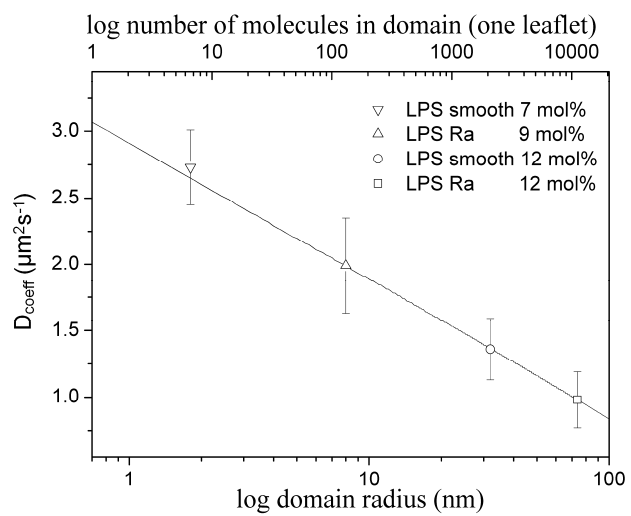


Figure S3.